Erschienen in: Physical Review B ; 95 (2017), 5. - 054411
https://dx.doi.org/10.1103/PhysRevB.95.054411

Thermally induced magnon accumulation in two-sublattice magnets

Ulrike Ritzmann
Institute of Physics, Johannes Gutenberg University Mainz, D-55099 Mainz, Germany
and Department of Physics, University of Konstanz, D-78457 Konstanz, Germany

Denise Hinzke and Ulrich Nowak
Department of Physics, University of Konstanz, D-78457 Konstanz, Germany

We present a temperature-dependent study of the thermal excitation of a magnon accumulation in two-sublattice magnetic materials. Using atomistic spin model simulations, we study the local magnetization profiles sublattice-wise in the vicinity of a temperature step in antiferromagnets, as well as in ferrimagnets. It is shown that the strength of the magnon accumulation in these systems scales with the derivative of the magnetization with respect to the temperature. These results give an insight into the complex temperature dependence of the magnon accumulation by making a direct link to the macroscopic behavior of the magnetization.

I. INTRODUCTION

The spin Seebeck effect (SSE) [1–3], which was discovered in 2008, describes the excitation of spin currents via thermal gradients. In the presence of a temperature gradient, net magnonic spin currents propagate from the hotter towards the colder direction. These currents can be detected in a metallic contact material using the inverse spin Hall effect [4]. These new techniques open up the possibility for new design concepts of thermoelectric applications including the interplay of heat, charge, and spin [5–7]. In previous years, a variety of experimental studies have been performed to investigate the characteristics of thermally excited spin currents, as the influence of the interface [8], the dependence on the thickness of the magnetic sample [9], and the influence of the temperature or external magnetic fields [10–14]. In recent experiments, it was shown that the SSE is significantly enhanced by using multilayer structures [15,16].

To describe these experimental findings, theoretical models have been developed [9,14,17–21]. These theories, based on magnonic spin currents as the origin of the SSE, cover some of the observed characteristics, for example, the thickness dependence of the effect. It was demonstrated experimentally that the measured spin Seebeck coefficient increases with increasing thickness for thin films and later saturates on a characteristic length scale. Due to a comparison of experiments and numerical simulation, this saturation effect can be referred to as a finite magnon propagation length [9]. Moreover, strong magnetic fields are used to control the SSE and suppress low frequency magnons of the excited spin currents. By performing atomistic spin model simulations, it has been shown that the contributions of the so-called subthermal magnons are much higher as expected, since the frequency dependent propagation length for these magnons is larger than the averaged magnon propagation length [14].

But the mentioned descriptions are based on a simplified ferromagnetic model. However, the most common material for the magnetic insulator in the SSE measurements is yttrium iron garnet (YIG), which is a ferrimagnetic material [22]. The observed complex temperature dependence of the SSE in YIG [10], as well as the observed magnetic field dependence indicate that the SSE depends on the frequency spectrum of the excited magnons. Therefore, a ferrimagnetic model is needed to include the complex frequency spectra of the magnons. A first theoretical model for SSE in antiferromagnets and compensated ferrimagnets in a two-sublattice material has been derived by Ohnuma *et al.* [23]. They claim that even if the SSE is vanishing for antiferromagnets, it is nonvanishing for compensated ferrimagnets. Moreover, in recent experiments in gadolinium iron garnet (GdIG) two sign changes of the spin Seebeck effect have been observed [24]. One sign change was observed at the compensation point of the magnetization.

In this paper, we study numerically the thermal excitation of magnonic spin currents by calculating the resulting magnon accumulation in two-sublattice materials in the vicinity of a temperature step. We consider two extended heat baths that are connected in the center of the longest axis. This temperature step provides a local source of a thermally induced spin current. We show with atomistic spin model simulations that, in agreement with earlier predictions, the magnon accumulation vanishes and no angular momentum is transferred. In ferrimagnetic systems with compensation point of the magnetization, we investigate the temperature dependence of the excited magnon accumulation and link the results with the difference of the equilibrium magnetization of the two heat baths as the driving force of the thermally excited magnon accumulation. This shows that even around the compensation point, at which the magnetization vanishes, a spin current can be excited.

II. METHODS

This work focuses on a numerical study of the thermally excited magnon accumulation in two-sublattice magnets. For that purpose, we model a simple cubic lattice with magnetic moments that can differ between the two sublattices A and B. We consider a Hamiltonian including exchange interactions with isotropic exchange coupling J_{ij} between the magnetic moments i and j and an anisotropy with an easy axis in the

z direction described by the anisotropy constant d_z, leading to

$$\mathcal{H} = -\sum_{i,j} J_{ij}\mathbf{S}_i\mathbf{S}_j - d_z\sum_i \left(S_i^z\right)^2. \tag{1}$$

Classical spin model simulations have been performed by solving the stochastic Landau-Lifshitz-Gilbert equation for each normalized magnetic moment $\mathbf{S}_i$ [25],

$$\frac{\partial \mathbf{S}_i}{\partial t} = -\frac{\gamma}{\mu_s(1+\alpha^2)}\mathbf{S}_i \times (\mathbf{H}_i + \alpha(\mathbf{S}_i \times \mathbf{H}_i)), \tag{2}$$

where γ is the gyromagnetic ratio, μ_s the magnetic moment, and α the phenomenological damping constant. The effective field $\mathbf{H}_i$ of each magnetic moment is given by

$$\mathbf{H}_i = -\frac{\partial \mathcal{H}}{\partial \mathbf{S}_i} + \boldsymbol{\zeta}_i(t). \tag{3}$$

The temperature is included as additive white noise $\boldsymbol{\zeta}_i(t)$ to the effective field. The noise terms fulfill $\langle \boldsymbol{\zeta}(t)\rangle = 0$ and $\langle \zeta_\eta^i(0)\zeta_\theta^j(t)\rangle = \mu_s/\gamma 2\alpha k_B T_p \delta_{ij}\delta_{\eta\theta}\delta(t)$, where η and θ denote the Cartesian components, k_B the Boltzmann constant, and T_p the temperature given by the lattice of the system. The numerical integration of the equations of motion for each normalized magnetic moment is very time consuming, but provides a correct temperature dependence of the magnetization and the full frequency spectra of the magnons without artificial cutoffs due to discretization effects.

In a first step, an antiferromagnetic system has been studied. In this case, the interaction of only nearest neighbors is considered and the exchange constant is given by $J_{ij} = J_{AB} < 0$. In a second step, the model is extended to a ferrimagnetic system with two different magnetic moments of the single sublattices, including also next-nearest-neighbor interaction. In both cases, the magnetic moments are initialized parallel or antiparallel to the easy axis in the z direction. We choose a geometry with the longest axis in the z direction with 512 magnetic moments and a small cross section. For the antiferromagnets we consider a cross section of 16×16 magnetic moments and for the ferrimagnets, we simulate a cross section of 32×32 magnetic moments. In the considered system, a time-independent temperature profile is applied, describing the lattice temperature of the systems. This profile includes a temperature step in the center along the longest axis of the system from the temperature T_1 to T_2.

Due to this temperature step, the magnetic system is in a nonequilibrium state. In the hotter heat bath exist more magnons than in the colder one. Therefore, a net magnon current from the hotter towards the colder region of the system is excited, as studied earlier for a ferromagnetic system [19]. The excited magnon current modifies the local magnon density and the magnetization and the system relaxes and reaches a quasistationary state, in which the local magnetization and the excited spin current are on average time independent.

Possible reflections of the excited spin current at the cold end of the system are suppressed by using absorbing boundary conditions implemented by an exponential increase of the damping constant close to the end of the system. In the following the resulting magnetization profiles in the different two-sublattice magnets are discussed.

III. MAGNON ACCUMULATION IN ANTIFERROMAGNETS

As a first step, the thermally driven nonequilibrium states in antiferromagnets have been investigated. In the considered antiferromagnet, the magnetization of the system is vanishing, since the magnetizations of the two sublattices compensate each other at every temperature. Therefore, a thermally excited magnon current would carry no spin and no magnon accumulation would be observed.

In order to visualize the transfer of angular momentum, the local magnetization in the quasistationary states is calculated as the average of the normalized magnetic moment $\mathbf{S}_i(t)$ over a time interval and over the x-y plane. Similar to the ferromagnetic case studied earlier [19], the local magnetization deviates from its equilibrium value m_0 close to the temperature step. These deviations are defined as magnon accumulation, given by

$$\Delta m(z) = m(z) - m_0(z). \tag{4}$$

To get a deeper insight, we calculate additionally the magnon accumulation in each sublattice. For that purpose the sublattice magnetization is determined and the sublattice magnon accumulation $\Delta m^{A,B}(z)$ in each sublattice is defined accordingly to Eq. (4) as the deviation of the local sublattice magnetization $m^{A,B}(z)$ from the equilibrium value $m_0^{A,B}$.

The results are shown exemplary in Fig. 1 for a system with $8 \times 8 \times 512$ magnetic moments with an anisotropy constant $d_z = 0.01|J|$ and a temperature step from $k_B T_1 = 0.1|J_{AB}|$ to $k_B T_2 = 0$ as illustrated in the upper part of Fig. 1. The used damping constant is $\alpha = 0.01$. The absolute value of the local magnetization $m^{A,B}(z)$ of the single sublattices is increased in the hotter region (decreased in the colder one) due to a lack (surplus) of magnons caused by the net magnonic current. This is illustrated in the middle part of Fig. 1.

In the figure below, the corresponding magnon accumulation for the sublattices is shown. The sublattice magnon accumulations appear only close to the temperature step and vanish with increasing distance from the temperature step. They have an opposite sign and additionally, a sign change appears at the temperature step. Nevertheless, the total magnon accumulation in the antiferromagnet is totally compensated, as proposed by Ohnuma *et al.* [23].

In a two-sublattice magnet with a cubic lattice, two magnon branches exist. Both branches can have different frequencies. For the two different modes, the precession of the single magnetic moments in the system are in the opposite direction. Due to reversed amplitude ratios of the sublattices, the two modes carry angular momentum with a different sign. In the absence of a magnetic field, the two magnon modes in the considered antiferromagnet are degenerated but carry opposite angular momentum of the same absolute value. The two modes are illustrated in Fig. 2. The single magnetic moments can precess in both directions around their effective field. Due to the effective torques acting on the magnetic moments, the amplitude of one sublattice is larger than that of the other leading to a transport of angular momentum due to the magnon modes. Due to their degeneracy, the magnon modes are excited thermally with the same probability. Hence, the magnon current excited in a temperature gradient do on

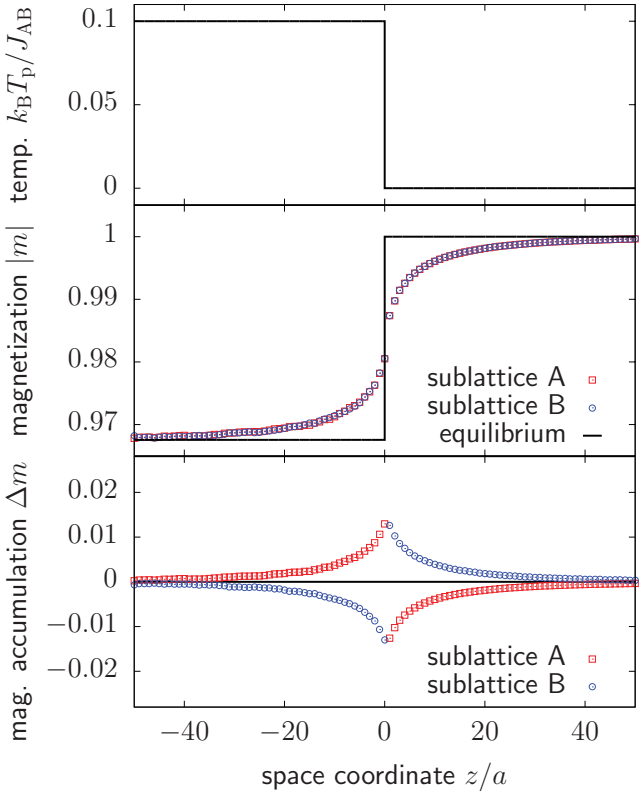

FIG. 1. Absolute value of the normalized magnetization m and the magnon accumulation Δm versus the space coordinate z of the single sublattices of an antiferromagnet around a temperature step exemplary for a damping constant of $\alpha = 0.01$, and an anisotropy constant of $d_z = 0.01J$.

average not transport angular momentum and the resulting total magnon accumulation vanishes.

Nevertheless, the thermally excited magnon current, which is visible in the single sublattices, transfers heat from the hotter towards the colder region, dependent on the damping in the system. These excited magnon currents can be used

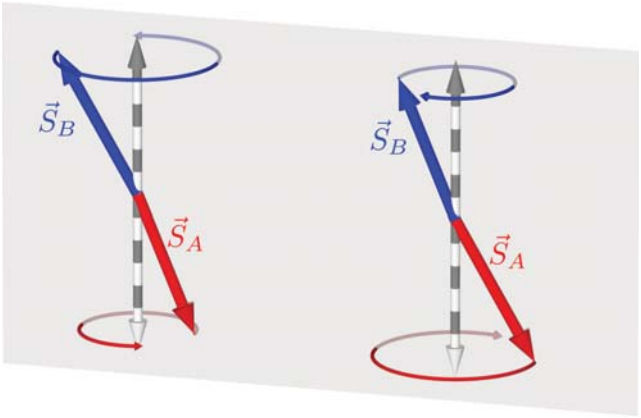

FIG. 2. Illustration of the two magnon modes in an antiferromagnet with degenerated dispersion relation. The magnetic moments of the single sublattices can either precess left- or right-handed leading to magnon modes transporting opposite angular momentum.

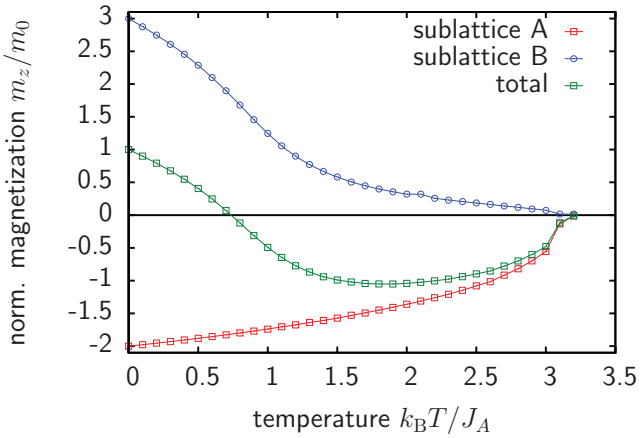

FIG. 3. Normalized magnetization component m_z/m_0 of the single sublattices A and B, and of the total system versus temperature T in thermal equilibrium.

for heat transfer in the system or to drive a domain wall [26,27]. Recently it has been shown that thermally driven domain walls in antiferromagnets can move much faster than in antiferromagnetic systems [28].

IV. MAGNON ACCUMULATION IN FERRIMAGNETS

In a next step, the thermal excitation of a magnon accumulation in a two-sublattice ferrimagnet with a magnetic compensation point is investigated. A first theoretical model by Ohnuma *et al.* shows a nonvanishing spin current at the compensation point [23], whereas in recent measurements by Geprägs *et al.* a sign change of the spin Seebeck coefficient in gadolinium iron garnet was observed [24]. In the performed measurements, the total magnetization of the sample is parallel to the external magnetic field. Therefore, the orientation of the magnetization of the sublattices changes and cause a sign change. Additionally, they found a second sign change at low temperatures. By studying the frequency spectra in thermal equilibrium at different temperatures, the authors explain this sign change by a compensation of the involved magnon modes.

In this paper, we consider a minimal model for a ferrimagnet including magnetic compensation. In this system, the second sublattice B has a larger magnetic moment than the sublattice A, but demagnetizes at lower temperatures due to the next-nearest neighbor interaction. We have chosen a lower intrasublattice exchange interaction for the second sublattice, $J_B < J_A$. In particular, we have chosen a ratio of the magnetic moments of the sublattices of $\mu_B = 1.5\mu_A$, and exchange constants of $J_B = 0.2J_A$ and $J_{AB} = -0.1J_A$. Here, the dominant exchange interaction term is given by the interaction of the magnetic moments of sublattice A [29].

The magnetization $\mathbf{m}$ is given as the averaged magnetic moment over the whole system. It can be written as $\mathbf{m} = \mu_A\langle\mathbf{S}_A\rangle + \mu_B\langle\mathbf{S}_B\rangle$. In thermal equilibrium at a temperature of $k_B T = 0$, the magnetization is given by $|m_0| = |\mu_A - \mu_B| = 0.5\mu_A$. The temperature dependence of the normalized equilibrium magnetization for this system is illustrated in Fig. 3. In this figure, only the z component of the averaged magnetization of the whole system is shown, aligned with the

easy axis of the model. The other two components vanish on average. Using the z component of the magnetization instead of its absolute value includes additionally the information about the direction of the magnetization. This plays an important role for the determination of the magnon accumulation around the compensation point, where the direction of the magnetization changes.

As shown in Fig. 3, the magnetization at low temperatures is aligned in the direction of the magnetization of sublattice B, since its magnetic moment is larger. But due to the lower exchange interaction of sublattice B, it demagnetizes at lower temperatures and the magnetization is compensated at a temperature of $k_\mathrm{B}T_\mathrm{comp} = 0.7J_A$ changing its direction. Finally, the magnetization vanishes at a critical temperature of $k_\mathrm{B}T_\mathrm{C} = 3.2J_A$.

In this system, we have investigated the thermally driven magnon accumulation in the vicinity of a temperature step dependent on the temperature level of the system. To resolve the magnon accumulation at high temperatures, we have used a system consisting of $512 \times 32 \times 32$ magnetic moments. This larger system leads to a huge computational effort of the performed simulations, but it enables us to average out thermal fluctuations and to detect local magnetization profiles with a high accuracy even at high temperatures. Moreover, we have calculated the average over four simulations to resolve even small magnon accumulations. This allows us to identify a sign change of the thermally created magnon accumulation at high temperatures.

We have studied, similar to the antiferromagnetic case, a system with a constant temperature step at the center of the z direction with a temperature difference of $k_\mathrm{B}\Delta T = 0.1J_A$ and a damping constant of $\alpha = 0.01$. Additionally, we have calculated the magnon accumulation due to this temperature step for different temperature levels. The resulting magnon accumulation in the quasistationary state of the system is shown exemplary for $k_\mathrm{B}T_2 = 0$ in the upper part of Fig. 4. As before, a net magnon current appearing due to the temperature gradient creates deviations from the equilibrium value. In the hotter region the number of magnons is reduced in comparison to the equilibrium situation and, therefore, the absolute value of the magnetization of the single sublattices is increased. In the cold region the situation is reversed and the additional magnons cause a reduction of the absolute value of the sublattice magnetizations.

This leads to the shown magnon accumulation of the single sublattices. In contrast to antiferromagnets, the total magnon accumulation, which is given as the sum over the contributions of the two sublattices, is no longer compensated. At low temperatures, it is dominated by the change of the magnetization of sublattice B.

By varying the used temperature level of the temperature profile, the total magnon accumulation shows a strong temperature dependence. This is illustrated for different temperatures in the lower part of Fig. 4. In the low temperature regime, the total magnon accumulation increases at first and shows a maximum close at the compensation point. In agreement with the predictions by Ohnuma *et al.* [23], the magnon accumulation does not change its sign at the compensation point, $k_\mathrm{B}T_\mathrm{comp} \approx 0.7J_A$. For even higher temperatures, the total magnon accumulation decreases and shows a sign change

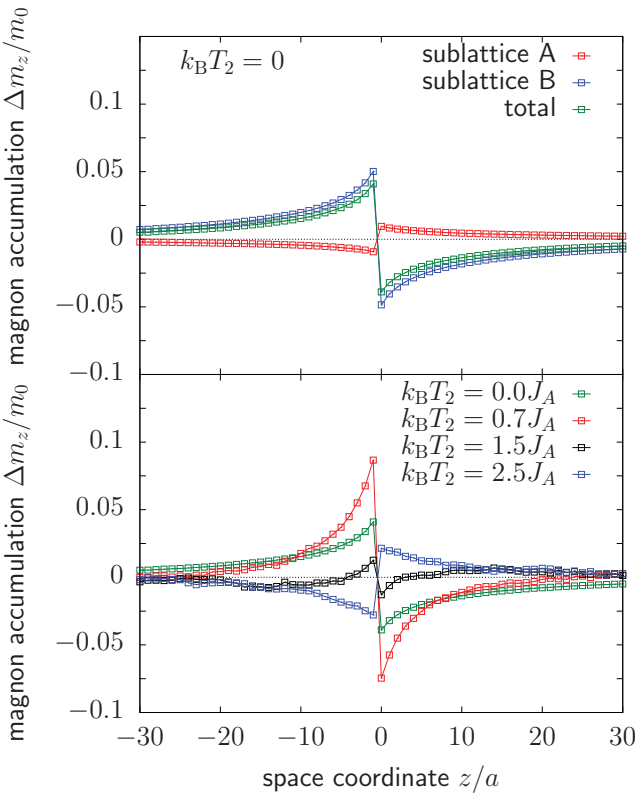

FIG. 4. Magnon accumulation due to a temperature step for different temperature levels. (Top) Magnon accumulation $\Delta m_z/m_0$ versus the space coordinate z of the single sublattices and the total magnon accumulation due to a temperature step. (Bottom) Total magnon accumulation $\Delta m_z/m_0$ versus the space coordinate z for different temperature levels T_2.

around a temperature of $k_\mathrm{B}T_2 = 1.8J_A$. The accumulation vanishes at the critical temperature.

Also in the two-sublattice ferrimagnet that is used, two magnon branches exist. In contrast to the antiferromagnet, the branches are not degenerated and they are thermally excited with different probabilities. The modes affect the magnetization of both sublattices, but dependent on the mode, the amplitude of each mode in one sublattice is larger than in the other defining the polarization of the mode. The lower frequency mode carries angular momentum proportional to $-m_z\mathbf{e}_z$. The higher mode carries the opposite angular momentum. In this case, the amplitude of the second sublattice is more affected.

The thermally excited spin current is given by the sum of the magnons from both branches. The strength of the total magnon accumulation of each magnon branch scales in first order with the difference of the magnon densities in the two heat baths. At low temperature, the total magnon accumulation is dominated by the contribution of the low frequency branch. An increase of the total magnon accumulation should therefore be due to an increase of the difference of the magnon densities of the low frequency branch. At higher temperatures, the higher branch becomes more important and the transported spin current is reduced since more and more magnons with opposite spin polarization are contributing. At a characteristic

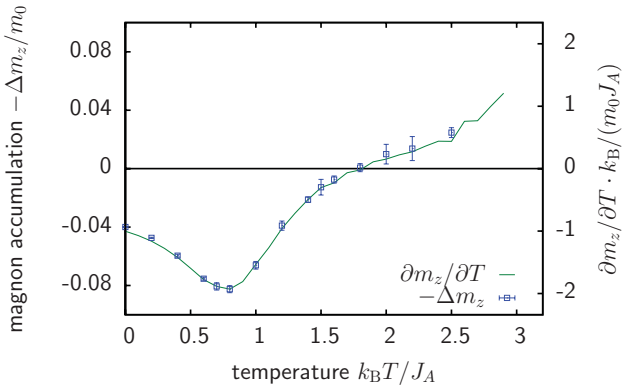

FIG. 5. Strength of the magnon accumulation $\Delta m_z(T)$ at the temperature step as a function of the temperature in comparison with the derivative of the magnetization with respect to the temperature $\partial m_z/\partial T$ as a function of the temperature T.

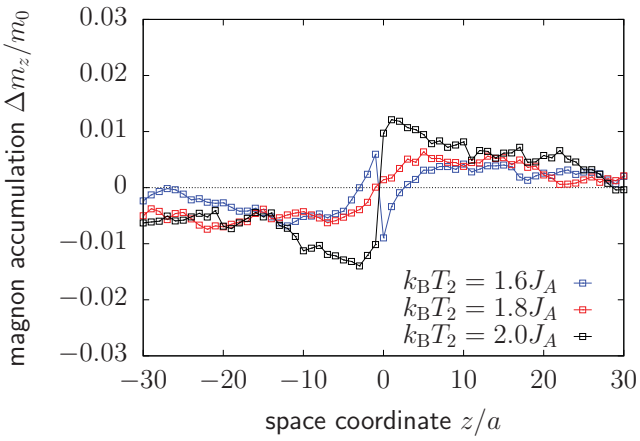

FIG. 6. Magnon accumulation due to a temperature step as a function of the position z for different temperature levels close to the compensation point of magnon accumulation.

temperature the contributions from the two branches cancel each other and the magnon accumulation vanishes. Above this temperature, the higher branch is dominating and the total magnon accumulation has an opposite sign.

This described temperature dependence of the total magnon accumulation can be linked on a macroscopic scale with the difference of the magnetization between the two heat baths. If the magnetization varies a lot with temperature, the magnon density of one or both magnon branches varies a lot. Therefore, one can assume that the total magnon accumulation scales with the derivative of the magnetization with respect to the temperature in thermal equilibrium.

In order to derive the derivative of the magnetization with respect to the temperature, $\partial m_z/\partial T$, numerically for the studied system, the difference quotient of the magnetization due to a temperature difference $\Delta T = 0.1 J_A$ is calculated up to the second order. To compare this derivative with the total magnon accumulation, the strength of the magnon accumulation directly at the temperature step is considered, which is defined by

$$\Delta m_z(T) = \tfrac{1}{2}(\Delta m_z(-a, T + \Delta T) - \Delta m_z(0, T)). \quad (5)$$

Assuming that the magnon accumulation is nearly symmetric around the temperature step, we use the full height of the jump of the magnon accumulation from the hotter towards the colder region and divide it by a factor of 1/2. The calculated derivative of the magnetization with respect to the temperature as well as the total magnon accumulation are shown in Fig. 5. The temperature dependence of both quantities shows a very good agreement over the whole temperature range. The total magnon accumulation at the temperature step scales linear with the gradient of the magnetization with respect to the temperature with a scaling factor of $\Delta m(0) \approx -23.4\ J_A/k_B \cdot \partial m_z/\partial T$. This scaling factor depends on system parameters as the damping constant α, since for lower damping more magnons propagate around the interface. Hence the strength of the total magnon accumulation at the temperature step is increased for lower damping.

This scaling explains the nonvanishing total magnon accumulation around the compensation point. Since the first sublattice demagnetizes at low temperatures, the magnetization varies a lot with temperature. This is still true at the compensation point and, therefore, the total magnon accumulation is around its maximum value. At higher temperatures, sublattice B is mainly demagnetized and the magnetization changes less with temperature and the strength of the total magnon accumulation decreases. Around a temperature of $k_B T_2 = 1.8 J_A$, the magnetization varies only weakly with temperature and the gradient as well as the total magnon accumulation vanishes. At even higher temperatures, the magnetization increases with temperature, leading to a gradient and a magnon accumulation with opposite sign.

Furthermore, we observe a sign change of the magnon accumulation at a temperature of $k_B T_2 = 1.5 J_A$ with increasing distance to the temperature step, as shown in Fig. 4. In Fig. 6, the total magnon accumulation for temperature levels around $k_B T_2 = 1.8 J_A$ are shown. According to the results shown in Fig. 5, the total magnon accumulation directly at the interface changes its sign around this temperature. Nevertheless, the sign of the total magnon accumulation far away from the temperature step is the same below and above the sign change of the magnetization slope. This can be explained by the different length scales for magnon propagation of the two different modes. If the involved magnons from the higher frequency branch have a higher propagation length than the magnons from the lower one, the relative contribution of the higher branch increases with distance to the temperature step and can even dominate. Hence, the sign of the magnon accumulation can change. The observations of this effect show that the magnon modes have different length scales. This could be measured, for example, in the so-called nonlocal spin Seebeck geometry that was studied recently for YIG [30–32].

V. SUMMARY

In this paper, we present a study of the excitation of thermally induced spin currents in two-sublattice materials by investigating the magnon accumulation that is induced due to a temperature step. We show in agreement with

earlier predictions by Ohnuma *et al.* [23] that in antiferromagnets the magnon accumulation and the corresponding spin current vanish. Nevertheless, in a compensated two-sublattice ferrimagnet the thermally induced magnon accumulation does not vanish around the compensation point.

By studying the sublattice-wise contributions of the magnon accumulation, we link the microscopic results with the macroscopic behavior of the magnetization, that can be measured experimentally. The observed magnon accumulation scales with the change of the magnetization with respect to a temperature change. By studying the temperature dependence of the magnon accumulation, we show a correlation between the slope of the magnetization and the strength of the magnon accumulation. Therefore, the maximum of the magnon accumulation appears at the inflection point of the magnetization curve, whereas the signal vanishes if the magnetization does not change with temperature.

This macroscopic link demonstrates that thermally excited spin currents are caused by a gradient in the magnon densities. In agreement with results in ferromagnets, also in ferrimagnets the gradient of the magnon densities cause a magnonic spin current. But in two-sublattice materials, both magnon branches have to be included, leading to a complex temperature dependence of the driving force of thermally induced spin currents. Using these results, one can identify new materials with high spin Seebeck coefficients in the preferred temperature range, by simply studying the temperature dependence of the magnetization.

ACKNOWLEDGMENTS

The authors would like to thank the Deutsche Forschungsgemeinschaft (DFG) for financial support via SPP 1538 "Spin Caloric Transport" and the SFB 767 "Controlled Nanosystem: Interaction and Interfacing to the Macroscale".

[1] K. Uchida, S. Takahashi, K. Harii, J. Ieda, W. Koshibae, K. Ando, S. Maekawa, and E. Saitoh, Nature (London) **455**, 778 (2008).
[2] K. Uchida, J. Xiao, H. Adachi, J. Ohe, S. Takahashi, J. Ieda, T. Ota, Y. Kajiwara, H. Umezawa, H. Kawai, G. E. W. Bauer, S. Maekawa, and E. Saitoh, Nat. Mater. **9**, 894 (2010).
[3] K. Uchida, H. Adachi, T. Ota, H. Nakayama, S. Maekawa, and E. Saitoh, Appl. Phys. Lett. **97**, 172505 (2010).
[4] E. Saitoh, M. Ueda, H. Miyajima, and G. Tatara, Appl. Phys. Lett. **88**, 182509 (2006).
[5] G. E. W. Bauer, E. Saitoh, and B. J. van Wees, Nat. Mater. **11**, 391 (2012).
[6] S. R. Boona, R. C. Myers, and J. P. Heremans, Energy Environ. Sci. **7**, 885 (2014).
[7] K. Uchida, M. Ishida, T. Kikkawa, A. Kirihara, T. Murakami, and E. Saitoh, J. Phys.: Condens. Matter **26**, 343202 (2014).
[8] Y. M. Lu, J. W. Cai, S. Y. Huang, D. Qu, B. F. Miao, and C. L. Chien, Phys. Rev. B **87**, 220409 (2013).
[9] A. Kehlberger, U. Ritzmann, D. Hinzke, E.-J. Guo, J. Cramer, G. Jakob, M. C. Onbasli, D. H. Kim, C. A. Ross, M. B. Jungfleisch, B. Hillebrands, U. Nowak, and M. Kläui, Phys. Rev. Lett. **115**, 096602 (2015).
[10] E.-J. Guo, J. Cramer, A. Kehlberger, C. A. Ferguson, D. A. MacLaren, G. Jakob, and M. Kläui, Phys. Rev. X **6**, 031012 (2016).
[11] T. Kikkawa, K. Uchida, S. Daimon, Y. Shiomi, H. Adachi, Z. Qiu, D. Hou, X.-F. Jin, S. Maekawa, and E. Saitoh, Phys. Rev. B **88**, 214403 (2013).
[12] T. Kikkawa, K.-i. Uchida, S. Daimon, Z. Qiu, Y. Shiomi, and E. Saitoh, Phys. Rev. B **92**, 064413 (2015).
[13] H. Jin, S. R. Boona, Z. Yang, R. C. Myers, and J. P. Heremans, Phys. Rev. B **92**, 054436 (2015).
[14] U. Ritzmann, D. Hinzke, A. Kehlberger, E.-J. Guo, M. Kläui, and U. Nowak, Phys. Rev. B **92**, 174411 (2015).
[15] R. Ramos, T. Kikkawa, M. H. Aguirre, I. Lucas, A. Anadón, T. Oyake, K. Uchida, H. Adachi, J. Shiomi, P. A. Algarabel, L. Morellón, S. Maekawa, E. Saitoh, and M. R. Ibarra, Phys. Rev. B **92**, 220407(R) (2015).
[16] K.-D. Lee, D.-J. Kim, H. Y. Lee, S.-H. Kim, J.-H. Lee, K.-M. Lee, J.-R. Jeong, K.-S. Lee, H.-S. Song, J.-W. Sohn, S.-C. Shin, and B.-G. Park, Sci. Rep. **5**, 10249 (2015).
[17] J. Xiao, G. E. W. Bauer, K. C. Uchida, E. Saitoh, and S. Maekawa, Phys. Rev. B **81**, 214418 (2010).
[18] S. Hoffman, K. Sato, and Y. Tserkovnyak, Phys. Rev. B **88**, 064408 (2013).
[19] U. Ritzmann, D. Hinzke, and U. Nowak, Phys. Rev. B **89**, 024409 (2014).
[20] S. R. Etesami, L. Chotorlishvili, A. Sukhov, and J. Berakdar, Phys. Rev. B **90**, 014410 (2014).
[21] S. M. Rezende, R. L. Rodr'iguez-Suárez, R. O. Cunha, A. R. Rodrigues, F. L. A. Machado, G. A. Fonseca Guerra, J. C. Lopez Ortiz, and A. Azevedo, Phys. Rev. B **89**, 014416 (2014).
[22] V. Cherepanov and I. Kokolov, Phys. Rep. **229**, 81 (1993).
[23] Y. Ohnuma, H. Adachi, E. Saitoh, and S. Maekawa, Phys. Rev. B **87**, 014423 (2013).
[24] S. Geprägs, A. Kehlberger, F. D. Coletta, Z. Qiu, E.-J. Guo, T. Schulz, C. Mix, S. Meyer, A. Kamra, M. Althammer, H. Huebl, G. Jakob, Y. Ohnuma, H. Adachi, J. Barker, S. Maekawa, G. E. W. Bauer, E. Saitoh, R. Gross, S. T. B. Goennenwein, and M. Kläui, Nat. Commun. **7**, 10452 (2016).
[25] U. Nowak, Classical spin models, *Handbook of Magnetism and Advanced Magnetic Materials* (John Wiley & Sons, New York, 2007), Vol. 2.
[26] S. K. Kim, Y. Tserkovnyak, and O. Tchernyshyov, Phys. Rev. B **90**, 104406 (2014).
[27] E. G. Tveten, A. Qaiumzadeh, and A. Brataas, Phys. Rev. Lett. **112**, 147204 (2014).
[28] S. Selzer, U. Atxitia, U. Ritzmann, D. Hinzke, and U. Nowak, Phys. Rev. Lett. **117**, 107201 (2016).
[29] F. Schlickeiser, U. Atxitia, S. Wienholdt, D. Hinzke, O. Chubykalo-Fesenko, and U. Nowak, Phys. Rev. B **86**, 214416 (2012).
[30] L. J. Cornelissen, J. Liu, R. A. Duine, J. B. Youssef, and B. J. van Wees, Nat. Phys. **11**, 1022 (2015).
[31] S. T. B. Goennenwein, R. Schlitz, M. Pernpeintner, K. Ganzhorn, M. Althammer, R. Gross, and H. Huebl, Appl. Phys. Lett. **107**, 172405 (2015).
[32] L. J. Cornelissen and B. J. van Wees, Phys. Rev. B **93**, 020403 (2016).